A DPD study of asphaltene aggregation: The role of inhibitor and asphaltene structure in diffusion limited aggregation

R. Skartlien[a,b], S. Simon[b], J. Sjöblom[b]

[a] *Institute for Energy Technology (IFE), P.O. Box 40, N-2027 Kjeller, Norway*
[b] *Department of Chemical Engineering, Ugelstad Laboratory, NTNU, N-7491 Trondheim, Norway*

Abstract

The kinetic effects of DBSA (Dodecyl Benzene Sulfonic Acid) and a linear amphihile on asphaltene aggregation was investigated, using Dissipative Particle Dynamics molecular simulations. The simulation results indicated that without inhibitor, diffusion limited asphaltene aggregation can be initiated by a kinetic/diffusive capture process between polar side chain groups rather than by interaction between polyaromatic rings. The most likely reason for this is that the side chains have higher diffusive mobility than the more massive aromatic ring structures. The DBSA acidic head groups adhered to the asphaltene side chain polar groups (the basic functional groups), resulting in lowered mobility of the side chain/DBSA complexes, thereby suppressing asphaltene aggregation initiation. A more mobile amphiphilic inhibitor without the aromatic ring gave a higher asphaltene aggregation rate. Adsorption of asphaltenes on a solid surface was suppressed with DBSA, due to an adsorbed monolayer of DBSA that occupied a significant fraction of the surface

Email address: roar.skartlien@ife.no (R. Skartlien)

area.

Keywords: asphaltene aggregation, diffusion limited aggregation, aggregation inhibitors, acid-base interaction, DPD simulation

---

1. Introduction

Asphaltene aggregation and precipitation can reduce oil recovery through plugging of rock pores, cause deposition in wells, clog pipelines and result in corrosion [1, 2, 3, 4, 5]. Asphaltenes stabilize water in oil emulsions by forming an interfacial layer that prevents coalescence between the water droplets [6]. Aggregation inhibitors are generally designed to prevent precipitation and/or deposition and it is of importance to identify the exact mechanisms that are responsible for aggregation between the asphaltene monomers, in order to design efficient inhibitor molecular structures. Furthermore, minimization of inhibitor concentration and environmental compatibility are also important issues to be addressed.

Asphaltenes are soluble in toluene but insoluble in n-alkane, and since they are the most polar components in petroleum crude oils, they adsorb easily onto hydrophilic (polar) substrates and on oil/water interfaces. It is generally accepted that the asphaltene polar groups are associated mainly to nitrogen, oxygen and sulphur that can be found in the polyaromatic ring structures (as heteroatoms) and in the side chains [7, 8, 9]. These groups enhance self-aggregation, precipitation and adsorption [10, 11]. Asphaltene precipitation in crude oil is also dependent on pressure [12], and for asphaltenes in model solvents, the aggregate sizes are reduced with increasing temperature [13].

The efficiency of an amphiphilic aggregation inhibitor is primarily controlled by the polarity or acidity of the head group and the length of the alkyl tail [14]. Increasing the polarity or acidity of the head group promotes the stability of asphaltenes, by increasing the interaction between the asphaltene functional (polar) groups and the head group of the inhibitor. When the tail length of the inhibitor is increased, the ability to stabilize the asphaltenes increases. When the carbon number of the tail is less than 6, the efficiency decreases significantly with decreasing tail length [14].

Dodecyl Benzene Sulfonic Acid (DBSA) has been used frequently to prevent aggregation and adsorption of asphaltenes [15]. DBSA shows an interaction with asphaltenes with predominantly basic functional groups but no interaction with asphaltenes with acidic groups[16]. DBSA is a relatively efficient inhibitor compared to other varieties such as nonylbenzene or alkylphenol [14], but it is only efficient at relatively high molar concentrations with several DBSA molecules per asphaltene. High molar concentration is however expected, in order to fully suppress the effect of the majority of functional groups in most of the asphaltene molecules.

For sufficiently high inhibitor concentration, the DBSA acid-base interaction enables dissolution of asphaltene aggregates in a non-polar solvent to a molecular solution with DBSA-asphaltene complexes, where DBSA acts as a solvation shell[17]. However, for lower inhibitor concentrations, flocculation between aggregates have been observed as a *result of* DBSA, where interactions between different ion pairs (AH+/DBS-) may cause flocculation into large aggregates, as measured by SAXS (Small Angle X-ray Scattering) [18]. Goual and Sedghi [15] argued that the electrostatic forces between such

ion pairs could result in filamentary aggregates in heptane/toluene mixtures (as visualized by transmission electron microscopy), since this did not occur with alkylphenol as inhibitor. Such aggregates may have fewer asphaltenes with than without inhibitor, but their total extent can be even larger than the original aggregate. Thermodynamic modelling supports this view [16]. Asphaltenes may also form micron-scale colloids which persist for a few minutes at a roughly constant size and then abruptly aggregate to a larger scale, on the order of ten microns[17].

In the current work, we focus on the "disintegration regime" at a sufficiently large inhibitor concentration and use heptane as solvent. The inhibition mechanisms may depend on the initial condition for the system; if the asphaltenes are fully dispersed when the inhibitor is added, or if the inihibitor is added after aggregates have formed. In the first case, inhibition will occur if the asphaltenes cannot capture each other efficiently due to a fast solvation process by DBSA. In the latter case, inhibition means that the aggregates are disintegrated dissolved by the inhibitor, by breaking the bonds between the asphaltenes. In order to maintain a dissolved state, it should again be essential that the capture mechanism between monomers is suppressed, which is the mechanism we have focused on in the current study.

Molecular simulations can be used as a guide to identify the inhibition mechanisms for any inhibitor. We have implemented a prototype DPD code for asphaltene simulations (DPD-SARA), that can also incorporate the additional molecules of the solvent and the inhibitor[19]. In feasible DPD simulations, the domain size ranges from $(10\ nm)^3$ on single CPU machines to $(100\ nm)^3$ on multi-CPU machines [20], with a few thousand to a few million

solute molecules, respectively. Typically 100 asphaltene molecules are used the domain, corresponding to the order of 100 000 ppm by weight, or 10-30 % wt (depending of the type of solvent). For comparison, crude oils have concentrations in the range $1-20\%$ (implying asphaltene aggregation in the bulk). We observe adsorption and aggregation, and this allows us to study the inhibitor effect that prevents formation of aggregates. The number of aggregates is however small due to the domain size limitations.

2. DPD model for DBSA and asphaltenes

In its original form, the DPD method was designed for treating physisorption processes due to van der Waals forces[21, 22]. Later extensions with Coloumb forces and electric fields have been implemented. Physisorption is regarded as the dominating mechanism for asphaltene adsorption and aggregation[23]. The acid-base reactions between the DBSA acid group and the asphaltene heteroatomic groups occur at relatively short distances below the Bjerrum length, and the relatively strong electrostatic interactions in the corresponding ion-pairs are accounted for qualitatively in our model by using relatively strong short range interactions in the simulation[24], rather than implementing the Coloumb force.

2.1. Equilibrium short range interaction versus long range electrostatics

In non-polar media, such as heptane, ion pairing between the protonated asphaltene (AH+) and the negative DBSA sulfonate (DBS-) ion is very strong, such that thermal energy alone cannot separate the ions if they are closer together than the Bjerrum length, which is about 30 nm in heptane. Within this radius, the electrostatic forces will provide the sufficient

binding energy. The interaction energy (between AH+ and DBS-), is an order of magnitude larger than asphaltene - alkylphenol (nonionic amphihile) interactions [15].

The oppositely charged components in the acid-base interaction constitutes a short range, strong electrostatic interaction. This is accounted for approximately by using relatively strong interactions (strong, net attraction via the DPD coarse grained force), without implementing the long range Coloumb force. It seems that this approach gives a qualitatively correct behavior in equilibrium situations with high DBSA concentrations where the asphaltenes are fully dissolved, and where the ionized DBSA and the asphaltenes are interacting only at short distance.

The potential energy of the long range dipole field between the ion-pairs is a factor of 5-10 smaller than the short range interaction [15]. However, it has been argued that aggregate flocculation can be induced by this long range electrostatic interaction between different bound ion pairs (AH+/DBS-pairs) [15]. Such long range effects will be neglected in the current work, thereby excluding the associated aggregate formation at moderate DBSA concentration.

A full treatment of Coloumb forces would have required a significant amount of implementation work by considering "wrap-around effects" of the electric field when using periodic boundary conditions (this is usually treated with Ewald summation methods), and the computational speed is then much reduced.

2.2. DPD and coarse grained molecules

The polyaromatic ring structure in the asphaltene core and the single aromatic ring in the DBSA molecule were treated numerically with Quaternion algorithms[1] to ensure that these structures rotate and translate as rigid objects while maintaining algorithmic simplicity [25, 26]. A detailed description of the basic DPD-technique can be found in the now extensive DPD literature [21, 22, 27, 28, 29]. In essence, the conservative part of the DPD forces between molecules i and j, $\mathbf{F}_{ij}^{C}$, is derived from a coarse grained interaction potential $U_{ij}(r_{ij}) = a_{ij}\mathcal{U}(r_{ij})$ between a pair of coarse grained DPD particles or "beads" (with a given functional form $\mathcal{U}$, and interaction parameter a_{ij}). This approximates the potential obtained by averaging over the underlying atomic structure, and over the different degrees of freedom (internal configuration, rotational angles, and relative positions in terms of the sub-groups of atoms that constitute the beads). The resulting coarse grained force is strictly repulsive due to a domination of the short range repulsive part of the van der Waals potentials. However, solute molecules can still attract each other and aggregate if their mutual repulsive force is lower than between the solvent and the solute.

The additional DPD parameters took their standard normalized values: $\gamma = 4.5$, $\tilde{\rho} = 3$, $\widetilde{kT} = 1.0$. We note that γ controls the viscosity of the system, $\tilde{\rho}$ is the normalized number density, and $\widetilde{kT}$ is the normalized kinetic temperature. A general normalized cutoff radius of $\tilde{r}_c = 1.0$ was set for the

[1] A quaternion is a complex number with one real part and three imaginary parts, which is used for tracking the orientation and rotation of the principal axis of the rigid aromatic ring structures.

conservative potential (beyond which the forces are set to zero). All DPD parameters are normalized using the standard definitions of the reference length and timescale [22].

2.3. Asphaltene, heptane and polar substrate DPD models

The asphaltene interaction parameters a_{ij} used in the current work were calculated by Zhang and coworkers [8][2]. Carbon and/or hydrogen in the asphaltene that are linked to a heteroatom of greater electronegativity (e.g., O, N or S), will form permanent electric dipoles. The presence of strongly electronegative heteroatoms in the ring structure and in the side chains will significantly increase the polarity and therefore increase the interaction with other polar groups, polar phases such as water, or polar sites on a mineral surface. The associated DPD interaction parameters have lower values, implying an attraction between these groups. Realistic aggregation behavior was obtained by Zhang et al. [8] by using a four-ring aromatic core with heteroatoms and polar side chains, and the aggregate sizes and internal organization (parallel stacking of the cores) was qualitatively similar to what is obtained from MD (Molecular Dynamics) simulations [7, 30].

The asphaltene model we implemented is visualized in Figure 1. Three different particle types, A,B,C was used to construct the asphaltenes. Type A refers to the individual H-C groups in the aromatic rings, B to CH_2 elements in the side chains, C to functional (polar) groups in the side chains (with the elements S,N, or O), and to polar heteroatomic groups in the aromatic rings (C=O bonds or HN groups). We chose four aromatic rings with two

[2]By application of the "Blends" package in Accelrys' Materials Studio.

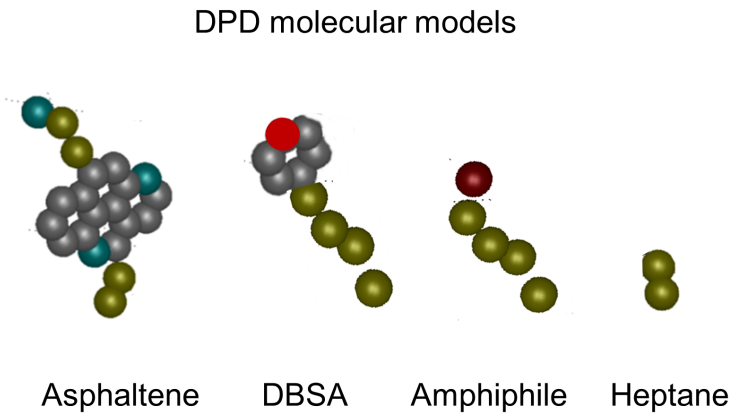

Figure 1: The coarse grained DPD molecular models. *Grey - type A*: hydrogen-carbon groups and carbon in aromatic rings. *Brown - type B*: alkyl side chain groups. *Blue - type C*: polar heteroatoms/functional groups. *Red - type D*: Acidic head group of the DBSA and the linear amphihile.

heteroatoms, and only two side chains to simplify the analysis. We found realistic aggregation properties also with two side chains. One side chain was short and apolar, consisting of two B-beads (B-B), and the other side chain was longer and had three beads (B-B-C) with a polar end bead.

Heptane (C_7H_{16}) was modelled with two beads of the B-type (B-B). For the mineral surface, we introduced one particle of type $\mathcal{S}$, to represent polar sites. These have affinity with the polar groups of the asphaltene (C-beads), and the head bead D of the inhibitors.

The interaction between the C-beads (side chain polar part and the heteroatoms) and the substrate $\mathcal{S}$ was taken to be relatively strong (a low value giving an attraction to the substrate), to obtain a clear effect from the polar groups. We adopted $a_{C\mathcal{S}}$=5, which is similar to the interaction parameter between polar groups in polymers and alumina substrates [31]. Similarly, the

interaction between the side chain polar groups was also relatively strong with $a_{CC} = 15$. The intra-bead binding forces in the side chains, and other molecular properties are discussed in more detail in our previous paper [19].

2.4. DBSA model, with extended interaction matrix

DBSA contains a single aromatic ring and an aliphatic chain with structure $(CH_2)_{11}CH_3 = C_{12}H_{25}$. The head group is that of sulfonic acid, $SO_2OH = SO_3H$, and this is attached to the aromatic ring on the opposite side of the chain anchor point (Figure 1). The alphatic chain was modelled with four B-beads ($4 \times 3 \times CH_2 = C_{12}H_{24}$), and the aromatic ring with A-beads as for the asphaltene. For simplicity (avoiding modification of the DPD code) we replaced one bead in the aromatic ring with a single head bead D, to represent the acidic group (red bead in Figure 1). The full (normalized) interaction matrix with extensions for the D-bead is

$$a_{ij} = \begin{pmatrix} & A & B & C & D & \mathcal{S} \\ A & 20 & 30 & 32 & 32 & 35 \\ B & .. & 26 & 45 & 45 & 55 \\ C & .. & .. & 15 & 5 & 5 \\ D & .. & .. & .. & 30 & 10 \\ \mathcal{S} & .. & .. & .. & .. & 0 \end{pmatrix}. \quad (1)$$

The effect of the DBSA head group on the asphaltene (effect of D on A,B) was chosen to be the same as the effect of the heteroatom group C on the asphaltene. The affinity between the D-bead and the heteroatoms was chosen to be relatively strong (a_{DC}=5), and stronger than the mutual heteroatom interaction (a_{CC}=15), to emulate the stronger electrostatic forces in the acid-

base pair. This choice for a_{DC} is consistent with colorimetric estimates of the interaction energies, as explained below.

The mutual D-D interaction is chosen to be weaker (a_{DD}=30), which will emphasize the asphaltene-DBSA interaction relative to the DBSA-DBSA interaction. Finally, the DBSA interaction with the polar substrate is chosen to be sightly weaker ($a_{D\mathcal{S}}$=10) than the heteroatom-substrate interaction ($a_{C\mathcal{S}}$=5), to not emphasize adsorption of DBSA over asphaltene adsorption.

2.5. The radial distribution function

The radial distribution function $g_{ij}(r)$ is used in the data analysis, and it is given by

$$n_{ij}(r) = g_{ij}(r)\bar{n}_j \tag{2}$$

where $\bar{n}_j$ is the average number density of molecule type j throughout the domain, and $n_{ij}(r)$ is the local number density of type j in a spherical shell of radius r, measured from the reference particle of type i. A larger maximum value of $g_{ij}(r)$ indicates more clustering of j molecules at a preferred distance from the particle i. For large radius, $g_{ij}(r \to \infty) = 1$, and n equals the average number density. The symmetry condition $g_{ij} = g_{ji}$ is valid for all particle pairs. The corresponding interaction energy (potential energy) per volume (J/m^3) is

$$E_{ij} = 2\pi\bar{n}_i \int_0^\infty r^2 U_{ij}(r) n_{ij}(r) dr = 2\pi\bar{n}_i\bar{n}_j \int_0^\infty r^2 U_{ij}(r) g_{ij}(r) dr. \tag{3}$$

The DPD potential is a "soft" quadratic potential

$$U_{ij}(r) = a_{ij}\frac{r_c}{2}\left[1 - \frac{r}{r_c}\right]^2, \tag{4}$$

which decays monotonically in the interval $[0, r_c]$ with a positive curvature $1/r_c$, and $U_{ij}(0) = a_{ij}r_c/2$ (U_{ij} is in units of Joule, and a_{ij} in units of Joule per meter when dimensionalized). Furthermore, r_c is the cutoff radius beyond which no forces are calculated so that $U(r \geq r_c) = 0$. The radial distribution function usually increases in the interval $[0, r_c]$.

2.6. Calorimetric estimate of the DBSA-asphaltene interaction energy

By using isothermal titration calorimetry (ITC), Wei et al. [32] measured the interaction energies between DBSA and synthetic model asphaltenes (named C5PeC11) in heptane/xylene mixtures. The model compound had 7 aromatic rings in the core, containing four oxygen and two nitrogen. One of the three side chains contained an HOOC group. The calorimetric measurements were calibrated to account for de-aggregation of the DBSA and the asphaltenes during injection into the solvent.

At a molar ratio DBSA/C5PeC11 in the range 2-3, the measurements indicated a dissociated state of the asphaltenes, with an interaction energy in the order of 10 kJ/mol (of DBSA), relative to a dispersed state of broken bonds between the asphaltenes (Figure 8 in Wei et al. [32]). However, the relative contributions from acid-base ion-pair interaction and H-bonding between the aromatic rings were uncertain. The electrostatic binding energy for ions separated by 1 nm is of the order of 30 kT [17], corresponding to 70 kJ/mol. Values in the range 10-80 kJ/mol have also been reported for these acid-base reactions[16]. Ring-interaction between C5PeC11 and DBSA due to H-bonding was estimated to 22.4 kJ/mol [32]. We assume that both H-bonding and acid-base reactions with the heteroatoms were involved, both contributing with 20-30 kJ/mol DBSA, corresponding to $33 - 50 \times 10^{-21}$J

per asphaltene heteroatom/DBSA pair (8-12 kT).

The interaction energy in DPD simulations has to be related to the interaction energy with the solvent. The corresponding net interaction parameter (normalized to the DPD units r_c and kT) is $\delta a = a_{BD}+a_{BC}-a_{DC} = (45+45-5) = 85$. The average interaction distance $\bar{r} \simeq r_c/2 \simeq 0.3$ nm, giving a characteristic potential energy of $U_{ij} \simeq (\delta a\ kT/r_c) \times \bar{r}/8 = 10.6\ kT = 42 \times 10^{-21}$J per interaction. This is consistent with the experimental estimates (8-12 kT). The energy scale kT of the DPD simulation was set at 290 Kelvin.

2.7. Linear amphiphilic model

The purpose of the linear amphiphile is to investigate the kinetic effects from removing the aromatic ting in the DBSA. Hence, the linear amphiphilic inhibitor is modelled with the same aliphatic chain and the same head group as for the DBSA, but with no aromatic ring (Figure 1). Hence, the chosen model is $D - B - B - B - B$, using the same interaction parameter matrix.

2.8. Initial conditions and resulting equilibrium configurations

A uniform well mixed distribution of asphaltene and inhibitor monomers (DBSA and linear chains, respectively) was imposed as an initial condition, wherefrom the system settled to an equilibrium state. It could be argued that aggregates usually already exist when inhibitors are added. The aggregates (including flocs/clusters) will then restructure or unravel once they interact with the inhibitor provided that the DBSA concentration is large enough (several DBSA per asphaltene) [17]. A new equilibrium state is then reached which is *likely* to be the same as the fully dispersed state that results from a well mixed initial condition. In this equilibrium state, the inhibitor

molecules form complexes with the asphaltenes that prevent the asphaltenes from aggregating.

2.9. Simulation setup

We used 100 asphaltenes, 400 inhibitors and 2000 heptane molecules in all cases. The size of the domain was set to $L_x \times L_z \times L_y = 8.1 \times 4.1 \times 16.3$ nm, with L_y being the domain size in the prependicular direction to the substrate (Figure 2). We used periodic boundary conditions in all directions for convenience, and the domain was cut in two by the substrate (Figure 2).

Initially, both the asphaltene and the solvent molecules were randomly and homogeneously distributed outside the substrate region. The simulations were run to thermodynamic equilibrium characterized by a constant kinetic temperature over time, and a fully developed (constant in time) concentration profile.

3. Diffusion limited aggregation and inhibition mechanisms

Diffusion limited aggregation (DLA) has been observed with continental model asphaltene compounds with a single large aromatic core and aliphatic side chains [34]. For asphaltenes taken from crude oil, Yudin et al. [33] found diffusion limited aggregation for moderate asphaltene concentrations below 3 g/L in toluene, but their results indicated reaction limited aggregation (RLA) at higher concentrations. It is noted that flocculation of asphaltene nanoaggregates is also controlled by DLA [35, 36].

The DPD framework is best suited for DLA-studies. The reason for this is that in standard DPD, there is no limiting timescale for the molecular interactions to occur (the probability of forming a permanent or temporary

bond upon collision between two DPD particles is unity). The only physical mechanism that can control aggregation initiation is therefore the relative diffusive motion between two different asphaltene molecules at large separation, and the mobilities of the different molecular segments (e.g. side chain, or polyaromatic ring structure) when two different molecules begin to interact physio-chemically at small separation. Once the asphaltenes interact (at a distance smaller than the interaction radius), it is the interaction forces that control the stability of the aggregates; stronger forces (polar interactions) reduces the probability of breaking the bonds, and the asphaltenes form permanent aggregates.

3.1. Mobility effects on aggregation

Increased mobility of a molecular segment corresponds to increased thermal velocity fluctuations; a lighter segment can "move around" more than a heavier one. Increased mobility of a section of a large molecule can then lead to increased probability of molecular interactions. From the simulations, it is evident that the side chains have larger mobility than the much heavier polyaromatic cores. The mobility μ can be defined in the conventional way,

$$D \equiv \mu kT \equiv \ell v_T, \tag{5}$$

where D is the associated diffusion coefficient, k is Boltzmanns constant, and T is the temperature. The diffusion length scale is defined by ℓ. The r.m.s thermal velocity fluctuation at temperature T decreases with the mass m of the molecular segment we consider,

$$v_T = \sqrt{\frac{3kT}{m}}. \tag{6}$$

The corresponding diffusion length over the duration t is

$$l_D \simeq \sqrt{6Dt}. \tag{7}$$

It is noted however, that the Brownian or thermal motion of a molecular segment (or a coarse grained DPD particle) that is bound to other segments is significantly constrained so that the mobility is reduced compared to that of a single free particle. The mobility related arguments we use are therefore only qualitative. In this context, it is important to note that the sigma bonding in the alkane side-chains allows for free rotation between the atoms, while the polyaromatic rings are more rigid.

The diffusion coefficient for a free DPD particle of mass m reproduces the fluid behavior of lowered diffusivity for higher particle mass and higher number density [37],

$$D = \alpha \frac{kT}{\gamma m n}, \tag{8}$$

where γ is the viscosity parameter, and n is the particle number density. The numerical factor $\alpha = 3/[w_D]$, involves the volume integral $[w_D]$ over the dissipative weight function $w_D(r)$[37]. Hence, the mobility in DPD simulations is

$$\mu = \frac{\alpha}{\gamma m n}, \tag{9}$$

and the corresponding diffusion length scale is $\ell = \alpha v_T/(3\gamma n)$. Individual DPD particles in the lighter side chains (of mass m) have a larger mobility (larger Brownian velocities) than the heavier aromatic ring structures (with mass $\simeq 6m$ for a single ring).

3.2. Aggregation mechanism without inhibitor

We studied some aspects of aggregation and adsorption with the same asphaltene model earlier [19], and we re-examine those results here. The heteroatom content in the aromatic cores was set to two polar atoms (as in Figure 1) or none (denoted by P/polar or A/apolar, respectively). The polar group in the side chain was present or replaced by a non-polar B-bead (again denoted by P and A). Thus, four combinations were used: polar chain and polar core (PP), polar chain and apolar core (PA), apolar chain and polar core (AP), and completely apolar asphaltene (AA).

A brief overview of the equilibrium aggregate structures as function of polar contents is given in Table 1, and Figure 2. For polar side chains (cases PP and PA), it appears that the aggregates are more well defined or dense (a larger number of asphaltenes in the aggregates for a given aggregate size) with aggregate sizes up to 4 nm, in contrast to apolar side chains (cases AP and AA). The heteroatom contents in the polyaromatic ring stucture plays only a minor role since cases PP and PA appear qualitatively similar in terms of nano-aggregate formation. This indicates that the presence of polar side chains is essential for capturing monomers onto the aggregates. The most likely reason for this is that the side chains are more mobile (less massive) than the polyaromatic rings, such that they can capture each other more efficiently (or with higher probability) than combinations involving the polyaromatic rings.

3.3. DBSA as aggregation inhibitor

DBSA model molecules were added to the PP-case where both the side chain and the polyaromatic core had polar groups. Aggregation was pre-

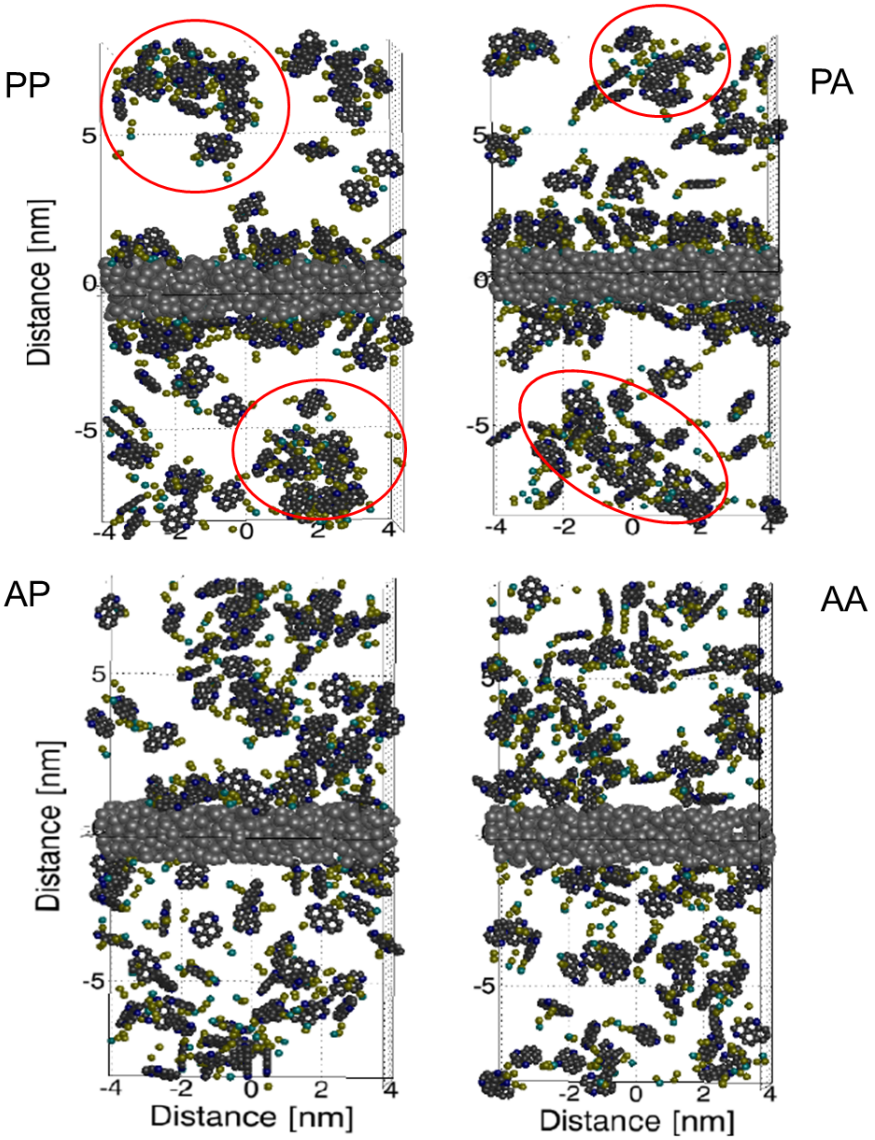

Figure 2: Nano-aggregation and adsorption in heptane as function of polar contents in the asphaltene. Efficient aggregation occurs when the side chains are polar (contains O, N, S heteroatoms), as in the upper two panels. Well defined aggregates are shown with red ellipses. The heteroatoms in the polyaromatic rings play only a minor role. The labels are defined as: polar chain and polar core (PP), polar chain and apolar core (PA), apolar chain and polar core (AP), and completely apolar asphaltene (AA). The polar substrate is placed in the middle of the domain (grey beads). The adsorbed amount is significantly larger when the side chains are polar. The same bead color coding is used for all cases.

(PP) **Polar chain, polar core**	(PA) **Polar chain, apolar core**
Well defined AG $\sim 2-4\ nm$	Well defined AG $\sim 2-4\ nm$
(AP) **Apolar chain, polar core**	(PP) **Apolar chain and core**
Loose AG $> 4\ nm$	No AG

Table 1: *Visual observation of aggregate structures.* AG = aggregates. Aggregates form when the side chain contains a polar group. Heteroatoms in the polyaromatic ring structure plays only a minor role.

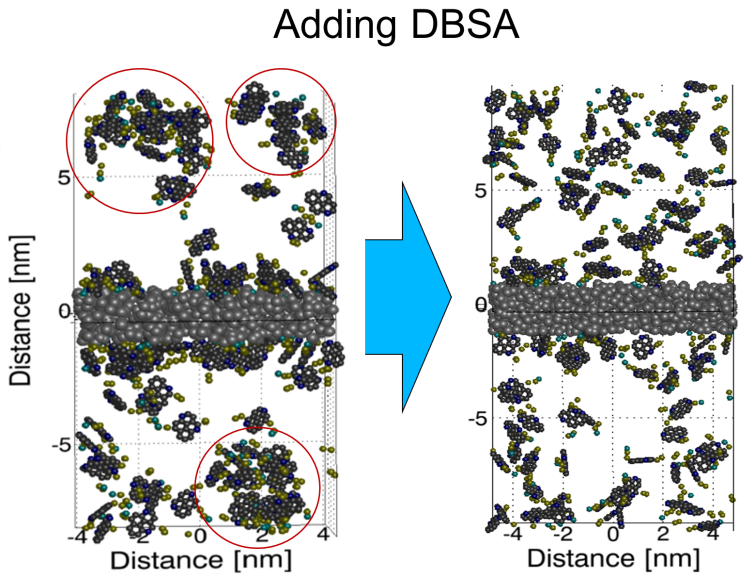

Figure 3: Adding DBSA to polar asphaltenes in heptane (the PP case), prevents aggregation. The DBSA molecules are not shown for clarity. The molar ratio DBSA/Asphaltene was 4.0.

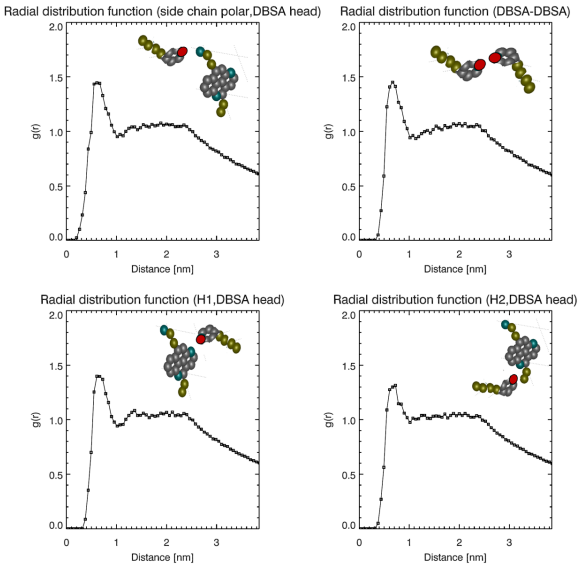

Figure 4: Radial distribution functions between the DBSA head and asphaltene heteroatoms, for the PP-case. The decline of the radial distribution function to values below unity at large distance is due to the finite size of the computational domain.

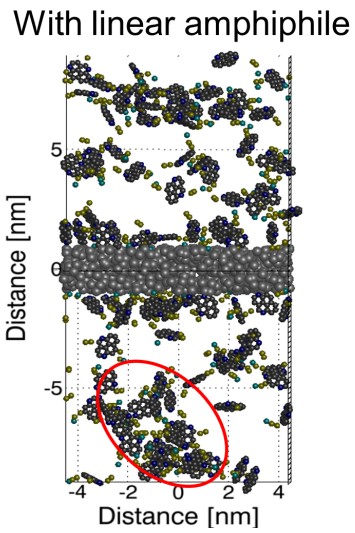

Figure 5: Adding linear amphiphile as inhibitor to the PP case. This inhibitor is much less efficient than DBSA. The linear amphihile has the same properties as the DBSA model molecule, but without the aromatic ring. The inhibitor is not shown for clarity, and the inhibitor mol-ratio is 4.0 also in this case (four per asphaltene).

vented with a molar ratio DBSA/asphaltene of 4.0 (four DBSA molecules per asphaltene molecule), as shown in Figure 3. The radial distribution functions g_{ij} for the interaction between the DBSA head group and the heteroatom sites including the side chain, and for the mutual interaction between the DBSA head groups, are given in Figure 4. Averaging of the data was performed only over a time interval where the system had settled to a steady state behavior (over the time interval $t \in 8000 - 15000$ in terms of simulation time steps).

The maximum value of all the radial distribution functions were comparable, although the preferred combinations were S.C.-DBSA (polar side chain group, and DBSA head group), and DBSA-DBSA (pairs of the DBSA head), with $Max(g) \simeq 1.5$. The probability of pairing up the heteroatoms in the polyaromatic core with the DBSA head was slightly less, with $Max(g) \simeq 1.3 - 1.4$. The side chain was more mobile than the polyaromatic component of the asphaltene so that the side chains may adhere with higher probability to the DBSA head, but this was evidently a minor effect. In conclusion, the DBSA seems to be roughly equally distributed among the four functional groups in the asphaltene model molecule.

Since the DBSA head group adheres to the asphaltene side chain polar group, it interferes with the capture mechanism between the side chains of the asphaltene, thereby suppressing asphaltene aggregation. The relatively massive aromatic ring of the DBSA reduces the mobility of the polar side chain /DBSA complex, and this is the likely reason for suppressing the capture probability between the asphaltenes.

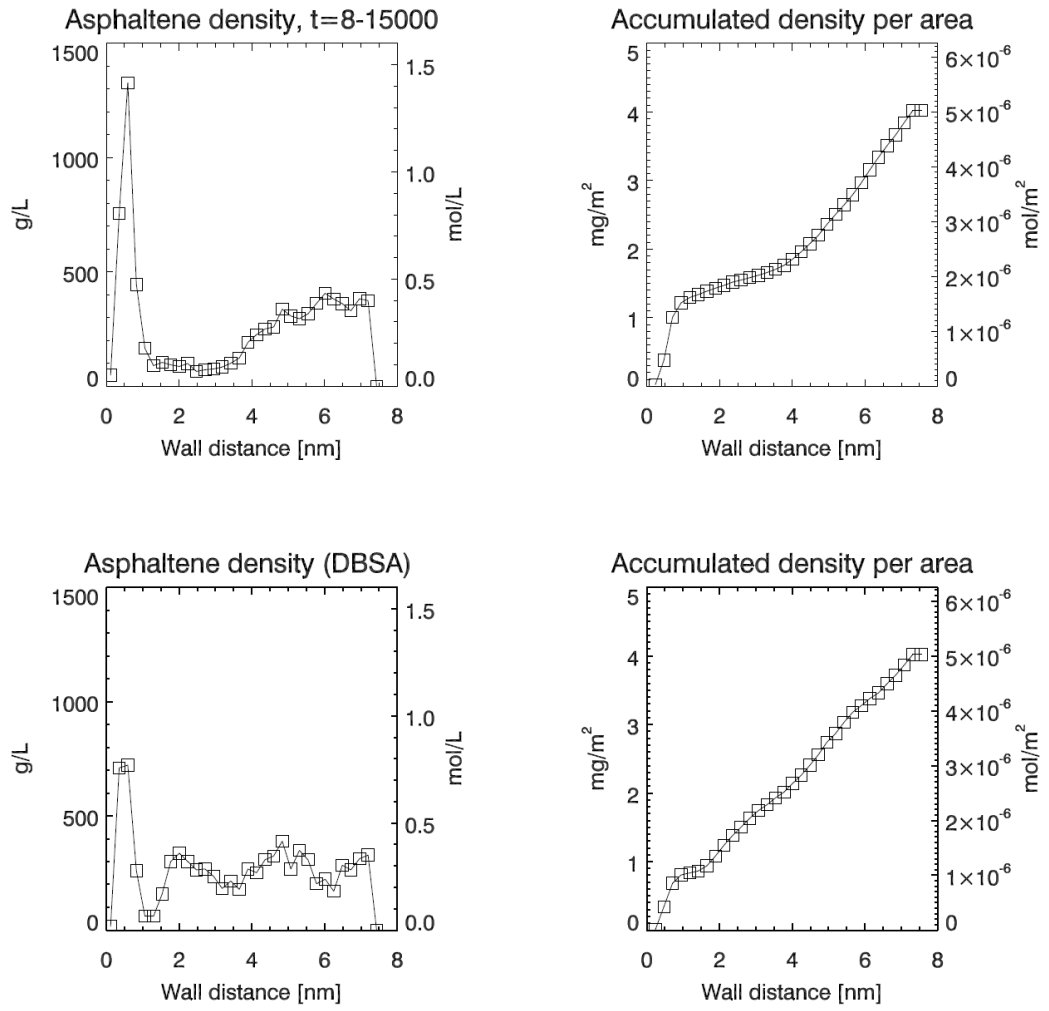

Figure 6: Density profiles for the PP case with DBSA. The left hand panels show the density profile for the asphaltene molecules. The right hand panels show the integrated surface density, starting from the wall. *Upper panels:* No inhibitor. The thickness of the adsorbed layer was about 1.5 nm, and the adsorbed surface density within this zone was about 1.3 mg/m^2 or 1.6×10^{-6} mol/m^2 (assuming an asphaltene molar weight of 800 g/mol). *Lower panels:* With DBSA. The adsorbed density is reduced to about 0.8 mg/m^2 or 1.0×10^{-6} mol/m^2.

3.4. Adsorption inhibition with DBSA

The equilibrium density profiles for the asphaltene molecules are shown in Figure 6. Again, averaging was performed over the time interval $t \in 8000 - 15000$, which represents an equilibrium state. DBSA decreased the adsorbed amount in the adsorbed layer between 0 and 2 nm from the surface (lower panels). The maximum asphaltene density in the adsorbed asphaltene layer was about 1400 g/L for heptane only (upper left panel) and about 700 g/L for DBSA and heptane (lower left panel). In all cases, we observed monolayer adsorption for both asphaltene and inhibitor. Monolayer adsorption of DBSA occupied a part of the surface area, making it unavailable to the asphaltenes so that the adsorbed density of asphaltenes was reduced.

Without DBSA, we obtained asphaltene surface densities in the simulation of 1-2 mg/m^2 (or around 2×10^{-6} mol/m^2). This compares well to experimental data of asphaltene adsorption on mineral surfaces, including calcite [38], and to monolayer adsorption on oil/water interfaces [39]. These surface densities correspond to significant lateral interactions between monomers with interaction energies that are comparable to asphaltene-substrate interactions, as discussed in our earlier work [19]. Since the lateral interactions are significant, organized structures that resemble those found in nanoaggregates in terms of $\pi - \pi$ stacking of the aromatic rings could be found. We did not analyze the details of reorganization of asphaltenes in the adsorbed layer due to DBSA, but we expect a more disorganized structure in this case.

3.5. Linear amphiphile as inhibitor

A linear amphiphile model was introduced to determine the role of the aromatic ring in the DBSA on aggregation efficiency. The inhibitor molar ratio was set to 4.0 also in this case. The linear amphihile had the same chemical properties as the DBSA (same acid group, and the same tail length), except for the aromatic ring. From mobility arguments, we would expect that a less massive structure without the aromatic ring would be a less efficient inhibitor since the amphiphile/asphaltene side chain complex would be less massive as well (hence, have higher mobility). Indeed, Figure 5 shows aggregation tendencies with the amphiphile as inhibitor.

Figure 7 shows the clustering of the asphaltene side chain polar groups without inhibitor, where the cluster density in terms of $Max(g)$ is 4.5 times larger than the average volume averaged density of the polar groups. The cluster density is strongly reduced with linear amphiphile ($Max(g) \simeq 2.5$), which indicates much looser aggregates. With DBSA, the cluster density is further reduced ($Max(g) \simeq 1.8$) and the aggregates vanish.

The radial distribution function that is associated with the interaction between the amphiphile head group and the asphaltene is shown in Figure 8. In this case the head group of the inhibitor showed a preferred affinity to the asphaltene side chain polar group, rather than head-head self-interaction. The maximum value $Max(g) \simeq 1.9$ for this combination, and 1.6 for the head-head interaction. The probability of pairing up with one of the heteroatoms in the polyaromatic core was significant $Max(g) \simeq 1.6$, although the probability was lower ($Max(g) \simeq 1.4$) for pairing up with the heteroatom closer to the anchor point of the non-polar side chain. In conclusion, the linear amphiphile

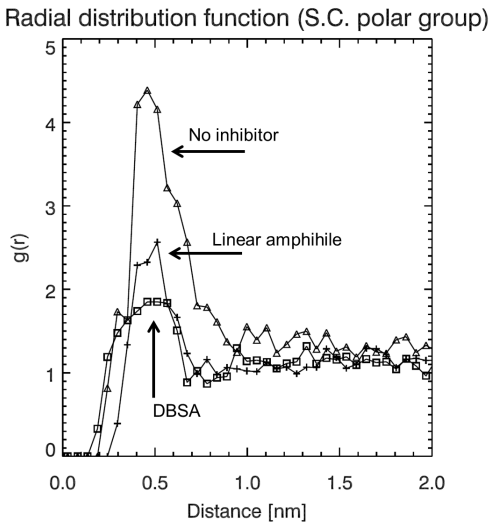

Figure 7: Radial correlation functions for the asphaltene side chain polar group. The polar component of the asphaltene side chain is clustered for no inhibitor (triangles). With DBSA, the polar group clustering almost vanishes (squares). With a linear amphiphile there is a weak tendency for clustering (crosses).

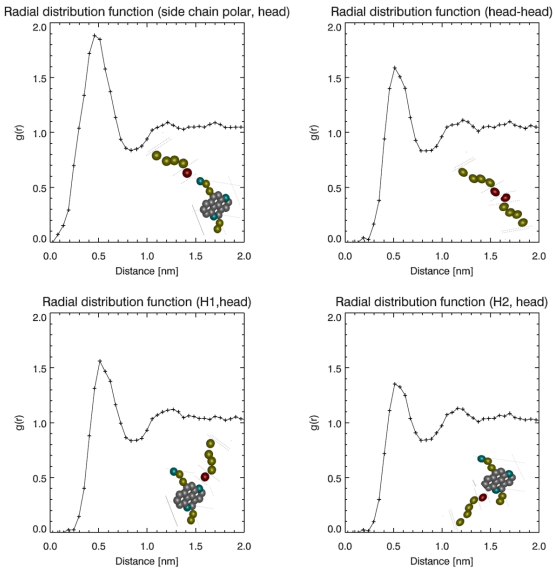

Figure 8: Radial correlation functions for the head group of the linear amphiphile and asphaltene heteroatoms. The amphiphile prefers the asphaltene side chain, rather than the heteroatoms in the polyaromatic core.

preferred to interact with the asphaltene side chain rather than with the heteroatoms in the polyaromatic core.

4. Discussion

Realistic aggregation patterns and $\pi - \pi$ interactions (polyaromatic ring-stacking behavior) in pure heptane were obtained with the chosen asphaltene related interaction parameters, as shown earlier [8, 19]. Nano-aggregates in the correct size range ($\sim$ 2 nm and above) formed without inhibitor, provided that the asphaltene side chains contained polar groups (with or without heteroatoms in the polyaromatic core). The nano-aggregates displayed internal $\pi - \pi$ stacking of the polyaromatic rings [8, 7, 30]. Without the

polar side chain groups, the aggregates were larger and above $\sim 4\ nm$ (with heteroatoms) or non-existent (without heteroatoms).

The most likely reason for aggregation *initiation* in our simulations (with polar side chain groups) is that the side chains are more mobile than the polyaromatic ring structure, such that they can capture each other more efficiently than a pair of polyaromatic rings. A capture process between a side chain polar group and a heteroatom in a polyaromatic ring is also a possible mechanism, but we consider such events to be less frequent, based on the combined mobility of the interaction pair.

The aggregate structures were completely disintegrated with the model DBSA molecule. The interaction energies between DBSA and asphaltenes that were used in the simulations were shown to be consistent with both theoretical and experimental estimates. The oppositely charged components in the acid-base interaction constitutes a short range, strong electrostatic interaction (within the Bjerrum length of about 30 nm at room temperature in heptane [17]). This interaction was accounted for in an approximate way by using relatively strong interactions between the DBSA head group and the asphaltene polar groups/heteroatoms in side chains and aromatic rings (a strong, net attraction via the DPD coarse grained force). This approach seems to give a qualitatively correct behavior in equilibrium situations at high DBSA concentrations where the asphaltenes are fully dissolved, and where the ionized DBSA and the asphaltenes interact only at short distance. The long range Coloumb force was not implemented.

The asphaltene-DBSA interaction was analysed in the view of fully dispersed DBSA monomers as an initial condition. However, self aggregation of

DBSA may play a role in asphaltene aggregation inhibition, through altered interaction between DBSA head groups and the asphaltene. Calorimetric measurements during titration of DBSA into xylene indicates self-aggregation into dimers for moderate concentration [40] (a possible mechanism being hydrogen bonding between the SO-H and the S=O group between the two DBSA head groups). The effect of DBSA aggregates on asphaltene aggregation could be detected as a slight change in the measured heat [40]. Also the DPD simulations displayed self interaction between the DBSA head groups, and we therefore consider the effect of such interactions to be incorporated at least qualitatively.

For nonylphenol (NP), the HO group on the aromatic ring is less acidic (pK_a around 9-10, compared to $pK_a < 0$ for DBSA) and the interactions with the heteroatomic basic groups are weaker. Fourier Transform Infrared Spectroscopy and Small-Angle X-ray Scattering Technique demonstrates that aggregate formation is more likely with NP than DBSA [18], indicating that acid-base reactions are important. The inhibition effect vanishes for nonylbenzene (NB), that does not have an acidic group [18]. Recent calorimetric measurements [32] indicate higher interaction energies between asphaltenes and DBSA than with NP, although these measurements do not distinguish between hydrogen bonding with $\pi - \pi$ interactions from acid-base interactions. The interaction with NP is much different than with DBSA, possibly involving more of the $\pi - \pi$ interactions between the NP aromatic ring and the polyaromatic structure of the asphaltene. We suggest that NP does not interact strongly with polar/basic side chain groups either, so that NP will not suppress the asphaltene side chain interaction to the same degree as for

DBSA, and aggregation initiation is therefore more likely with NP than with DBSA.

5. Conclusion

The simulation results without inhibitor demonstrated that the presence of polar groups in the asphaltene side chains is an important element in aggregation initiation from a fully dispersed state. The most likely reason for this is that the asphaltene polar side chains are more mobile than the heavier polyaromatic rings in the asphaltenes, so that these polar groups can capture each other with higher probability via diffusion (Brownian motion). Subsequent molecular interaction within aggregates lead to $\pi - \pi$ stacking between the polyaromatic cores [19], in order to minimize the potential energy in the final equilibrium state.

The DBSA molecule was found to be an efficient inhibitor since it strongly suppresses the mobility of the asphaltene polar side chain groups. In order to maintain an equilibrium state in situations where the inhibitor fully dissolves the aggregates, it should again be essential that the same side chain related capture mechanism between asphaltene monomers is suppressed.

Self-aggregation was prevented completely at a molar fraction (DBSA/ asphaltene) of 4. The DBSA acidic group paired up with the asphaltene heteroatoms in the core and in the side chains. The DBSA aromatic ring added relatively high mass to the asphaltene side chain when the acidic group paired with a basic functional side chain group. This reduced the mobility of the side chains (now a side chain-DBSA complex), which again reduced the capture probability between asphaltene monomers. An amphiphile with the

same acid character and same tail length as DBSA, but with no aromatic ring, resulted in some aggregation in accordance with this mobility mechanism.

The adsorption of asphaltenes onto a polar substrate was reduced with DBSA due to monolayer adsorption of DBSA that occupied some of the surface area, making it unavailable to the asphaltene polar groups. Without inhibitor, the polar side chain groups of the asphaltene (rather than the heteroatoms in the polyaromatic core) anchored to the substrate, as we discussed earlier [19].

Acknowledgments

This activity was a part of the JIP-project: "Improved Mechanisms of Asphaltene Precipitation, Deposition and Fouling to Minimize Irregularities in Production and Transport – A Cost Effective and Environmentally Friendly Approach", funded by The Research Council of Norway, BP (British Petroleum), Canadian Natural Resources Limited, Nalco Champion Technologies, Petrobras, Statoil ASA, Total, AkzoNobel and NTNU. Per-Erik Hellberg of AkzoNobel provided additional guidance on general inhibitor properties. The simulation model DPD-SARA was developed as a part of the Center for Research based Innovation FACE, funded by The Research Council of Norway, Statoil ASA, ConocoPhillips Scandinavia A/S, VetcoGray Scandinavia A/S, SPTgroup AS, FMC technologies, CD-adapco, and Shell Technology Norway AS.

References

[1] Vafaie-Sefti, M., Mousavi-Dehghani, S. A. (2006) Fluid Phase Equilib., 247: 182-189.

[2] Cruz, J. L. M. d. l., Arguelles-Vivas, F. J.; Matias-Perez, V.; Duran-Valencia, C. d. l. A.; Lopez-Ramirez, S. (2009) Energy Fuels, 23: 5611-5626.

[3] Drummond, C., Israelachvili, J. J. (2004) Pet. Sci. Eng., 45: 61-81.

[4] Buckley, J. S.; Liu, Y. J. (1998) Pet. Sci. Eng., 20: 155-160.

[5] Akbarzadeh, K.; Hammami, A.; Kharrat, A.; Zhang, D.; Allenson, S.; Creek, J.; Kabir, S.; Jamaluddin, A.; Marshall, A. G.; Rodgers, R. P.; Mullins, O. C.; Solbakken, T. (2007) Oilfield Rev., Summer 2007: 22-43.

[6] Harbottle, D.; Chen, Q.; Moorthy, K.; Wang, L. X.; Xu, S. M.; Liu, Q. X.; Sjoblom, J.; Xu, Z. H., (2014) Langmuir, 30: 6730-6738.

[7] Kuznicki, T., Masliyah, J.H., Bhattacharje, S. (2008) Energy and Fuels 22: 2379-2389.

[8] Zhang, S.-F., Sun, L.L., Xu, J.-B., Wu, H., Wen, H. (2010) Energy and Fuels, 24: 4312-4326.

[9] Sjöblom, J., Simon, S., Xu, Z., (2015) Advances in Colloid and Interface Science 218: 1-16.

[10] Adubu, A., Goual, L. (2009) Energy Fuels, 23: 1237-1248.

[11] Xing, C., Hilts, R. W., Shaw, J. M. (2010) Energy Fuels, 24: 2500-2513.

[12] Guo B, Song S., Chacko J., Ghalambor A., in "Offshore Pipelines" (2005) Elsevier Inc. ISBN:0-7506-7847-X.

[13] Espinat, D., Fenistein, D., Barre, L., Frot, D., Briolant, Y., (2004) Energy & Fuels 18: 1243-1249.

[14] Chang, C-L and Fogler, H.S., (1994) Langmuir 10:1749-1757.

[15] Lamia Goual, L., Sedghi, M., (2015) Journal of Colloid and Interf. Science 440: 23-31.

[16] Rogel, E., (2011) Energy Fuels 25: 472-481.

[17] Hashmi, S. M., Zhong, K. X., Firoozabadi, A. (2012) Soft Matter 8: 8778-8785.

[18] Chang, C-L and Fogler, H.S., (1994) Langmuir 10:1758-1766.

[19] Skartlien, R., Simon, S., Sjöblom, J., (2016) Journal of Dispersion Science and Technology 27:866-883.

[20] Wang, S., Xu, J., Wen, H. (2014) Computer Physics Communications, 185(12): 3069-3078.

[21] Hoogebrugge, P. J. and Koelman, K. M. V. A. (1992) Europhysics Letters, 19: 155-160.

[22] Groot, R. D. and Warren, P. B. (1997) J. Chem. Phys., 107(11): 4423-4435.

[23] Gonzalez, G.; Travalloni-Louvisse, A. M. (1993) SPE Production & Facilities 8(2): 91-96.

[24] Li, N.K., Fuss, W.H., Yingling Y.G. (2015) Macromol. Theory Simul 24: 7-12.

[25] Fincham, D. (1981) CCP5, Information Quarterly, 2: 6.

[26] Fincham, D. (1992) Mol. Simul., 8: 165.

[27] Espanol, P. and Warren, P. (1995) Europhysics Letters, 30: 191-196.

[28] Noid, W. G., Chu, J-W., Ayton G. S. (2008) Journal of Chemical Physics, 128: 244-144.

[29] Noid, W. G., Liu, P., Wang Y. (2008) Journal of Chemical Physics, 128: 244-115.

[30] Teklebrhan, R. B., Ge, L., Bhattacharje, S., Xu, Z., Sjöblom, J. (2012) J. Phys. Chem. B 116: 5907-5918.

[31] Kacar, G., Peters, E. A. J. F. and de With, G. (2013) J. Phys. Chem. C, 117: 19038-19047.

[32] Wei, D., Simon, S., Barriet, M., Sjöblom, J. (2016) Colloids and Surfaces A: Physiochem. Eng. Aspects: in press.

[33] Yudin, I.K., Nikolaenko, G.L., Gorodetskii, E.E., Markhashov, E.L., Agayan, V.A., Anisimov, M.A, Sengers, J.V. (1998) Physica A. 251: 235-244.

[34] Breure, B., Subramanian, D., Leys, J., Peters, C. J., Anisimov, M. A. (2013) Energy and Fuels 27: 172-176.

[35] Anisimov, M. A., Yudin I .K., V. Nikitin, G. Nikolaenko, A. Chernoutsan, H. Toulhoat, D. Frot, and Y. Briolant, (1998) J. Phys. Chem. 99: 9576-9580.

[36] Yudin I .K., G.L. Nikolaenko, E.E. Gorodetskii, V.I. Kosov, V.R. Melikyan, E.L. Markhashov, D. Frot, Y. Briolant, (1998) J. of Petr. Sci. and Eng. 20: 297-301.

[37] Marsh, C. A., Backx , G., Ernst M. H. (1997) Phys. Rev. E 56(2):1676-1691.

[38] Dudasova, D., Simon, S., Hemmingsen, P. V., Sjöblom, J. (2008) Colloids and Surfaces A: Physiochem. Eng. Aspects:317:1-9.

[39] Pradilla, D., Simon, S., Sjöblom, J. (2015) Colloids and Surfaces A: Physicochem. Eng. Aspects 466: 45-56.

[40] Wei, D., Orlandi, E., Simon, S., Sjöblom, J., Suurkusk, M. (2015) J. Therm. Anal. Calorim. 120:1835-1846.